

# Do physicists stop searches too early? A remote-science, optimization landscape investigation.

Robert Heck,<sup>1</sup> Oana Vuculescu,<sup>1</sup> Jens Jakob Sørensen,<sup>1</sup> Jonathan Zoller,<sup>2</sup> Morten G. Andreasen,<sup>1</sup> Mark G. Bason,<sup>3</sup> Poul Ejlersen,<sup>1</sup> Ottó Elíasson,<sup>1</sup> Pinja Haikka,<sup>1</sup> Jens S. Laustsen,<sup>1</sup> Lærke L. Nielsen,<sup>1</sup> Andrew Mao,<sup>1,4</sup> Romain Müller,<sup>1</sup> Mario Napolitano,<sup>1</sup> Mads K. Pedersen,<sup>1</sup> Aske R. Thorsen,<sup>1</sup> Carsten Bergenholtz,<sup>1</sup> Tommaso Calarco,<sup>2</sup> Simone Montangero,<sup>2,5</sup> and Jacob F. Sherson<sup>1,\*</sup>

<sup>1</sup>*ScienceAtHome, Department of Physics and Astronomy, Aarhus University, Aarhus, Denmark*

<sup>2</sup>*IQST, Ulm University, Ulm, Germany*

<sup>3</sup>*Department of Physics and Astronomoy, University of Sussex, Falmer, Brighton, United Kingdom*

<sup>4</sup>*Microsoft Research, New York, New York, USA*

<sup>5</sup>*Theoretische Physik, Universität des Saarlandes, Saarbrücken, Germany*

(Dated: September 8, 2017)

Despite recent advances driven by machine learning algorithms, experts agree that such algorithms are still often unable to match the experience-based and *intuitive* problem solving skills of humans in highly complex settings. Recent studies have demonstrated how the intuition of lay people in citizen science games [1] and the experience of fusion-scientists [2] have assisted automated search algorithms by restricting the size of the active search space leading to optimized results. Humans, thus, have an uncanny ability to detect patterns and solution strategies based on observations, calculations, or physical insight. Here we explore the fundamental question: Are these strategies truly distinct or merely labels we attach to different points in a high dimensional continuum of solutions? In the latter case, our human desire to identify patterns may lead us to terminate search too early. We demonstrate that this is the case in a theoretical study of single atom transport in an optical tweezer, where more than 200,000 citizen scientists helped probe the Quantum Speed Limit [1]. With this insight, we develop a novel global *entirely deterministic* search methodology yielding dramatically improved results. We demonstrate that this “bridging” of solution strategies can also be applied to closed-loop optimization of the production of Bose-Einstein condensates. Here we find improved solutions using two implementations of a novel remote interface. First, a team of theoretical optimal control researchers employ a *Remote* version of their *dCRAB* optimization algorithm (*RedCRAB*), and secondly a gamified interface allowed 600 citizen scientists from around the world to participate in the optimization. Finally, the “real world” nature of such problems allow for an entirely novel approach to the study of human problem solving, enabling us to run a hypothesis-driven social science experiment “in the wild”.

Keywords: citizen science | optimal control | quantum physics | ultracold atoms | closed-loop optimization | human problem solving | collective problem solving

## I. INTRODUCTION

In modern scientific research, high-tech applications, such as quantum computation [3], require exquisite levels of control while taking into account increasingly complex environmental interactions [4]. At the same time, addressing emergent phenomena such as global sustainable development challenges [5] requires interdisciplinary collaboration and appropriate mixtures of domain-specific methodologies. Across the natural and social sciences, finding good solutions to complex problems can be viewed within the unifying mathematical framework of a search problem over a non-convex high-dimensional function with many local optima. This concept of search within a *fitness landscape* emerged as early as the 1930s in biology [6], and has become a ubiquitous modeling tool across disciplines including evolutionary biology [7], physics [1, 8–10], computer science [11], management

[12], and anthropology [13]. Generally, search can be approached with local or global optimization methods. Local solvers are analogous to greedy hill climbers. They are efficient, but all solutions within a *basin of attraction* fall into the same local optimum and are therefore locally trapped. The global methods attempt to escape these basins by taking stochastic steps outside, which typically increases the runtime dramatically compared to the local solvers.

Achieving the proper balance between these is often referred to as the exploitation/exploration trade-off in both machine learning (ML) [14] and social sciences [15].

As global search algorithms effectively rely on *random jumps*, much effort in computer science is focused on developing algorithms that exploit the topology of the landscape to adapt search strategies and make better-informed jumps [11, 16–19]. Machine learning algorithms have achieved success across numerous domains, however, there is a growing effort to return to the subject’s roots (i.e. the study of human cognition) [20] by increasingly learning from human behavior and psychology in order to realize truly domain-general artificial

---

\* Electronic address: sherson@phys.au.dk

intelligence. The necessity of human input is demonstrated by the fact that the impressive advances in the field of (deep) neural network ML in recent years have not only arisen due to the increasing computational power and algorithmic advances, but also due to the increasing availability of massive human-labeled data sets [21]. Thus, as more systems of *human-machine hybrid intelligence* [2, 22] emerge, a critical challenge in the future will be the development of efficient techniques for people to take advantage of ML algorithms and an increased understanding and application of the value of the uniquely human contribution.

One approach to harness this potential contribution stems from the emerging field of citizen science [25]. Despite the common perception of humans as error-prone agents, there is a rapidly growing range of projects enabling people to solve problems that are beyond the capabilities of current computer algorithms. The concept of “games with a purpose” and the field of *human computation* have demonstrated many novel approaches for combining human and machine problem solving [26–29]. More recently, the creativity and intuition of non-experts have made an impact across different fields such as quantum physics [1], astrophysics [30, 31] and computational biology [32–34]. Often, citizen scientists are able to jump across very rugged landscapes and solve non-convex optimization problems efficiently using search methodologies that are difficult to encode in a computer algorithm.

On [www.scienceathome.org](http://www.scienceathome.org), our online citizen science platform, more than 200,000 people have so far contributed to the search for novel solutions to fast, 1D single atom transport [1]. Surprisingly, player solutions bunch into distinct groups (clans). Here we refer to such a group of related solutions all employing the same underlying physical intuition as a strategy. In the current work we pose the general question: Are established strategies in physics truly distinct, or are they simply labels we attach to different points in a continuum of possible solutions due to our inability to probe the entire solution space? In the latter case, coupled with the human desire to create identifiable patterns, this might cause us to terminate our search and prevent us from discovering the true global optimum. This premature termination of search nicely illustrates the *stopping problem* [35, 36] considered in both computer algorithms and social science. Random jumps in global search lead to potentially unbounded running time and therefore often require a decision to stop searching when the best solution so far is deemed “good enough”. A large body of literature has proposed analytic solutions for certain small, well-defined problems [35]. However, for large complex problems no analytic solutions exist and heuristics are instead required. For decades, the field of judgment and decision making has studied how humans employ *satisficing*, a heuristic that decision makers employ to stop searching after reaching an acceptable threshold [37]. How human decision makers determine these thresholds is a subject of intense debate [38].

Here, we explore the stopping problem and the possible uniqueness of identified strategies (clans) in terms of the topology of the *fitness landscape*: a function  $J(\vec{u}) \in \mathbf{R}$  given by the control variables  $\vec{u} \in \mathcal{S}$ , where  $\mathcal{S}$  is the set of possible solutions. Proving that a given solution is locally optimal involves extensive numerical work in either random sampling or systematic reconstruction of the full Hessian in the surrounding high-dimensional space [39]. In contrast, the same can be disproven simply by identifying a path of monotonously increasing yield in the landscape connecting it to another solution, which we shall denote a *bridge*. The topology of the fitness landscape depends critically on the choice of *parametrization* or *representation*. Figure 1a) illustrates a simple example of a challenging landscape which exhibits a negative curvature along the two orthogonal directions indicated with red lines and appears *neutral*, i.e., it has a flat plateau along a mixed direction. The bridge illustrated in figure 1a) by the blue dashed line could potentially be detected using random sampling combined with methods like principal component analysis [40]. However, if the bridge only exists along a certain axis and is very narrow it may become prohibitively complex to find as the number of dimensions grows.

Extending our previous research on the gamified atomic transport problem [1], we here investigate the uniqueness of the identified solution strategies by introducing the heuristics (a practical but not guaranteed optimal solution method) to explore along the high-dimensional vector connecting two distinct strategies. Surprisingly, we locate a narrow connecting bridge of high fidelity solutions. This demonstrates that for this problem a continuum of solutions with no clear physical interpretation can in fact be traced out if all hundreds of control variables are changed synchronously in the appropriate way. We employ this knowledge of the structure of the control landscape to introduce, to the best of our knowledge, the first quantum realization of a global search methodology without any random component and demonstrate clear improvements compared to previous citizen science based and purely numerical search strategies [1].

Despite the growing examples of successful citizen science projects, the field has been criticized for not yielding transferable insights. Here we demonstrate such transfer by applying the topological insights above to the optimization of an ultracold atom experiment located at Aarhus University. Starting with four distinct, conventional strategies, which each appear locally optimal (with respect to single parameter variations), we demonstrate that bridges can again be identified. We then locate novel, higher yield strategies by performing a more extensive search of the parameter space using a remote control software named Alice [41] in two unconventional ways (see figure 1c). First, we realize the first cloud-based, closed-loop optimization of such systems by establishing a real-time, remote connection to the basis-adaptive numerical search algorithm *RedCRAb*, developed and run-

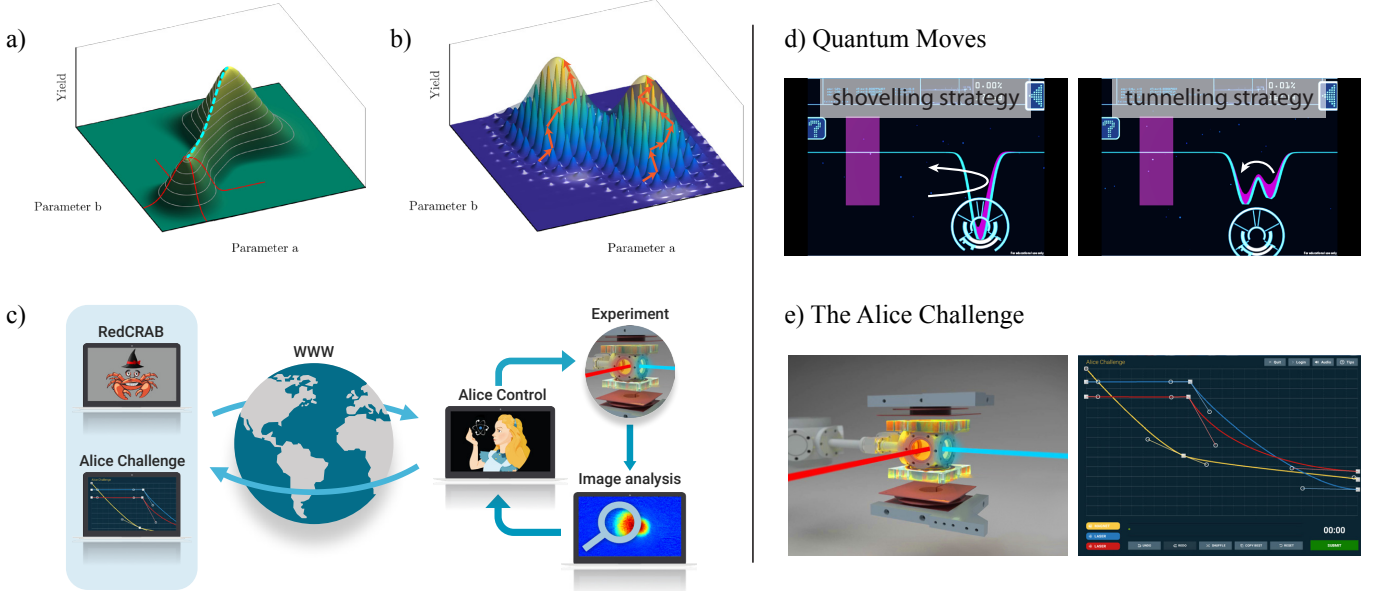


Figure 1. The topological concepts explored and the three remote-science investigations. a) Simple illustration of a non-trivial optimization landscape for two parameters denoted  $a$  and  $b$  demonstrating a topological feature that can complicate search in higher dimensions. Search only along an orthogonal set of directions, depicted by the red lines, may imply local optimality. To escape such a local trap, new search directions, or linear combinations of existing ones, have to be introduced which might enable one to find a *bridge* (blue, dashed line) leading to the global optimum of the landscape. If such a bridge is narrow and exists only along a specific direction it becomes increasingly difficult to identify with growing dimensionality of the optimization problem. b) Illustration of the concept of the *superlandscape*. Whereas the underlying optimization landscape consists of densely lying local optima, the superlandscape is defined as the smooth envelope function spanned on top of them. The two orange paths visualize the optimization with the GOLSS scheme by moving along the local optima of the underlying landscape towards an extremum in the superlandscape (for more details, see text). c) Remote scheme for RedCRAB and the Alice Challenge. The respective remote clients send experimental parameters through an online cloud interface which are turned into experimental sequences and executed by the Alice control program. The number of atoms in the Bose-Einstein condensate ( $N_{\text{BEC}}$ ) serves as fitness value and is extracted from images of the atom cloud taken at the end of each sequence. The Alice control program closes the loop by sending the resulting  $N_{\text{BEC}}$  back to the remote clients through the same cloud interface. d) Screenshots from Quantum Moves (see text for details). e) Screenshots of the *Alice Challenge* [23]. The left panel is a frame of the instructional video. Players can control the magnetic field gradient depicted by the yellow shaded coils and the two dipole beams in red and blue. The control happens in a client programmed with the cross-platform engine *Unity* [24] (right panel) and features a spline editor for shaping the ramps for which the same color coding was used.

ning at the University of Ulm. Second, we create an online gamified interface allowing 600 citizen scientists to contribute to the experimental optimization over a three week period.

Finally, we demonstrate that our experimental setup allows for a hypothesis driven social science investigation into how citizen scientists are able to solve challenging natural science problems. In this step towards massively controlled, online social science experimentation, we lay the groundwork for circumventing major issues that currently plague many problem solving studies in social and cognitive science: artificially designed, small problems [42] based on relatively small scale studies with paid participants [43] from a demographically biased participant pool [44].

## II. THEORETICAL OPTIMIZATION OF SINGLE PARTICLE TRANSPORT

In the following we briefly review the theoretical framework for gamified investigation of single atom transport in a controllable potential at the quantum speed limit (QSL) [1]. The framework is the citizen science game *Quantum Moves* [45] and in particular the specific level *Bring Home Water* (BHW) (see figure 1d). Here a graphically illustrated wavefunction of an atom in one dimension ( $|\psi\rangle$ ) must be collected from a static Gaussian shaped potential well (optical tweezer) and subsequently transported into the ground state within a designated target area. To realize this, the player dynamically adjusts the depth and position of a transport tweezer. The fraction of the state in the target state (the motional groundstate,  $|\psi_T\rangle$ ) is given by the fidelity  $0 \leq F \leq 1$  defined as  $F = |\langle\psi_T|\psi\rangle|^2$ . The player must also reach this state as quickly as possible (promoted by the introduc-

tion of a time penalty in the game). Due to constraints in available resources, computer-based optimization at the QSL exhibits exponentially growing complexity [1, 46]. Solutions to this particular challenge are valuable, for example for the realization of a large scale quantum computer based on ultracold atoms in optical lattices [47] and optical tweezers [48].

The focus in quantum optimal control has been primarily on developing tailored local optimization algorithms like Krotov, GRAPE and CRAB [49–52]. The former two methods are very efficient, since they exploit the structure of the Schrödinger equation, whereas CRAB is universally applicable since it can use a gradient-free method to reach the optimum, and furthermore it has the attractive feature of operating in a reduced sized basis, i.e. the search is performed in a reduced dimensional space. Recently, gradient-based optimization in a reduced basis has also been exploited in the GOAT and GROUP algorithms [53, 54]. All these local methods are typically turned into global optimizers by restarting over a wide range of initial seeds until they give sufficiently good results. In alternative efforts, global search methods such as Differential Evolution, CMA-ES, and reinforcement learning have been applied directly to quantum control [46, 55, 56] and very recently the local and global methods have been combined [54].

In Ref. [1] it was shown that the optimization of player solutions from the BHW challenge outperforms such purely numerical approaches for transport durations close to the QSL. The best results were found by optimizing the player solutions using the Krotov algorithm in a hybrid Computer-Human Optimization (CHOP). In order to compare the different solutions obtained with CHOP, a distance measure was introduced. A clustering analysis revealed that solutions fall into two distinct clusters denoted as “clans”. The solutions forming a clan all follow a similar strategy, to which one can assign a physical interpretation. One of the clans exploits quantum tunneling, while the members of the other clan use a classically inspired shoveling strategy [1]. The two strategies are depicted in figure 1d).

Here, we ask if these clans really represent physically distinct strategies in the sense that no mixed-strategy, high-yield solutions exist. Given the high dimensionality of the problem, an exhaustive exploration of the whole space is impossible to realize with a reasonable amount of time and resources. Instead, we investigated the topology of the landscape spanned by linear interpolation between the individual controls of representatives of the two clans. Given the interpolation parameter  $\alpha \in [0, 1]$ , the interpolated control is defined as

$$\vec{u}_{\text{int}}(\alpha) = \alpha \vec{u}_1 + (1 - \alpha) \vec{u}_2, \quad (1)$$

where  $\vec{u}_1$  and  $\vec{u}_2$  are the controls of the two solutions interpolated between. Figure 2a depicts a 2D visualization of the landscape corresponding to the interpolated solutions and local random perturbations to these using the

t-SNE algorithm [57] as applied in Ref. [1]. The rapid decline in fidelity of the interpolated points and the multitude of points yielding zero fidelity suggests that the clans can be seen as extremely small regions of good, nearly optimal solutions in the underlying optimization landscape.

According to this interpretation, one would expect local optimization of these solutions to drag them towards either the shoveling or the tunneling optimal solutions and thereby yield a region of attraction for each clan. Instead, local optimization using the Krotov algorithm results in the high fidelity *bridge* shown in figure 2b. In our numerical optimization, the displacement in terms of the distance metric [58] of each optimized solution from the initial seed is fairly small: the optimization of the points in figure 2a leads to nearly vertical lines in the visualized landscape. This implies that as long as the right region of the landscape is explored, very close to the non-perfect trial solution lies a better solution. Additionally, each initial seed converged to a different optimum, i.e., new, distinct solutions have been found as illustrated by the yellow points of figure 2b. Thus, the landscape is locally very rugged, but rich in optima. Physically, we interpret the sharpness of the peaks and the density of optima in terms of the population along the different instantaneous eigenvalues of the problem. Due to the time-energy uncertainty relation, rapid transfer in the vicinity of the QSL can only be achieved by significant excitations, which ensure rapid relative phase evolution of the individual wave function components [59]. Towards the end of the process the population needs to be refocused into the ground state. Any minor perturbation to a path at some instant will in general lead to a decreased fidelity. However, it can (nearly) be compensated with another carefully chosen perturbation at another time, leading to many closely spaced locally optimal solutions.

The fact that a single 1D-line scan identifies a bridge is an illustration of a deeper underlying principle in numerical optimization: whereas nearly all of the many possible search directions yield poor behavior (illustrated by the blue and red points in figure 2a), once a good heuristic encapsulating the essence of the problem is determined, low dimensional search is sufficient [60] (i.e., along the ridge of figure 1a).

Given the density of locally optimal points, we now define the *superlandscape* as the approximately smooth envelope function spanned by the optimal points. If  $\mathcal{O}$  is a local optimization algorithm then this landscape is the composition  $\tilde{J} = J[\mathcal{O}[\vec{u}(t)]]$ . Figure 1b) illustrates a simple, generic superlandscape. The underlying landscape consists of a dense collection of individual peaks with smoothly varying heights. The fidelity of a particular set of controls ultimately depends on the physical subprocesses (in this case excitations, phase evolution, and de-excitation). In most cases, it is reasonable to assume the fidelity to vary smoothly with variations in the subprocesses and we therefore conjecture the superlandscape (for this and many other physical processes)

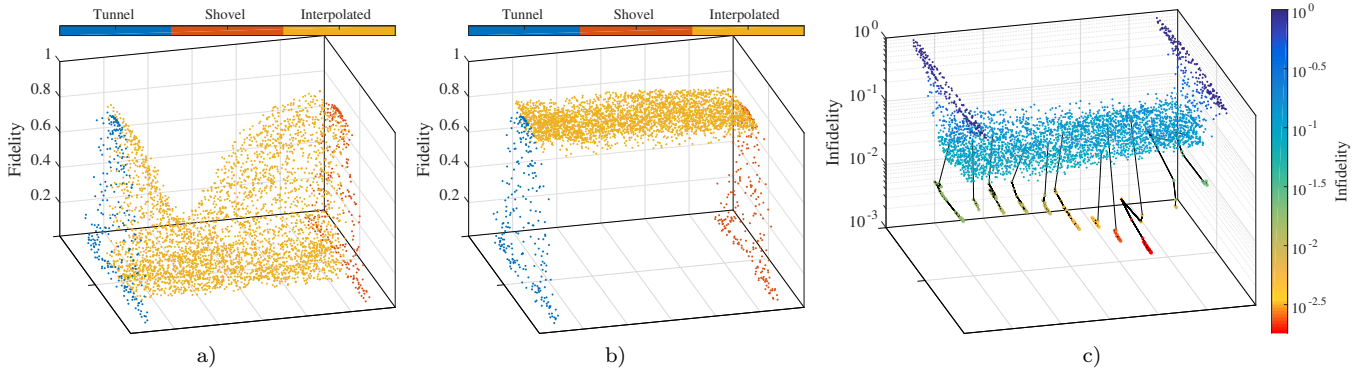


Figure 2. Visualization of the construction of a *bridge* between the two clans of solutions of the BHW game. The process time was set to  $T = 0.19$  (for a definition of units see [1]), which is below the estimated QSL for both tunneling and shoveling clans ( $T = 0.25$  and  $T = 0.20$  respectively). The colors in a) and b) denote the type of each solution. Note that for representation, the dimensionality has been reduced to two. Therefore, distances on the two horizontal axes should not be seen absolute and axes labeling was omitted. a) The result of using convex combinations of solutions and local perturbations of them to establish a connection between the two clans is shown. b) Local Krotov optimization was applied to the yellow marked points in a) and close-to-optimal solutions are attained. c) Infidelity of resulting optimized solutions. Starting from the established bridge from a), individual points were optimized using the GOLSS scheme (black, nearly vertical lines).

to be smooth over sufficiently small scales. If the superlandscape can be evaluated with sufficient speed (using efficient local optimization) then we propose to perform completely deterministic global optimization using a method that we call Gradient-Optimization and Local Superlandscape Search (GOLSS). Such a hybrid local-local optimization scheme has been recently proposed in the context of trap-free landscapes in the presence of noise [61]. In contrast, GOLSS entirely eliminates the random steps normally present in global optimization and could therefore potentially offer significant speedup compared to existing methods. In the illustration of 1b), this means that GOLSS is able to deterministically jump between local optima of increasing quality towards an extremum in the superlandscape, as exemplified by the two orange paths. They illustrate that the superlandscape itself is not necessarily free from local optima.

Here, we use a Nelder-Mead type search [62] to implement GOLSS. We start this optimization of  $\tilde{J}$  at a number of interpolated solutions along the located bridge. This results in significantly improved solutions as shown in figure 2c. These solutions are found at a duration of  $T = 0.19$ . The best optimized solutions from this combined search reached  $F = 0.998$  in fidelity, which is an improvement of nearly two orders of magnitude in terms of infidelity over the best player optimized solution (CHOP) yielding  $F = 0.929$ . It also represents an improvement of the previously obtained numerical estimates of the QSL for both the tunneling and shoveling clans, which were at  $T=0.25$  and  $T=0.20$  respectively. When we inspect the actual solution it is clearly seen to be a combination of the tunneling and shoveling strategies, since it places the transport tweezer on top of the atom rather than to the left or right of it.

These results demonstrate that although the full prob-

lem has an intractable dimensionality often there exist simple seed spaces of high quality. Previously, in Ref. [1], we constructed these search spaces explicitly using parametrizations that emerged from data analysis of large amounts of numerical solutions. Recently, a similar approach was applied to extract low-dimensional search spaces for spin-chain dynamics using ML-generated data [46]. The search along convex linear combinations of existing solutions introduced here may provide a computationally inexpensive methodology to identify promising search directions in the multidimensional landscape. In addition, we believe that the concept of superlandscape and local search within it will be a useful metaheuristic for finding high quality solutions for quantum optimal control problems.

### III. BOSE-EINSTEIN CONDENSATES IN DIFFERENT TRAP GEOMETRIES

Inspired by the theoretically well defined problem of the BHW challenge, the results of the analysis are applied to an ultracold quantum gas experiment. In these types of experiments, a dilute gas of atoms has to be cooled from a few hundred °C to a few hundred nK. A crucial step in this process is evaporative cooling [63] to a Bose-Einstein condensate (BEC). Typically, the atoms are initially captured and held in traps created by magnetic fields and tightly focused laser beams. Subsequently, the depth of the trap is lowered so that the hottest atoms can escape and the remaining cloud rethermalizes at a lower temperature. Although these dynamics are classical and not quantum, it is still sufficiently difficult to model so as to constitute a high-dimensional, complex optimization problem. Without a full model of the system, special-

ized optimal control algorithms like the previously used Krotov algorithm are not applicable. Additionally, the cooling of the atomic cloud, and thereby the evaluation of a single set of candidate controls, takes, in our case, about 35 s, which again puts severe constraints on the choice of optimization method.

Discovering optimized experimental sequences for ultracold quantum gas experiments has been investigated over the past decade by employing global closed-loop optimization strategies using genetic algorithms [64–67]. However, due to the random component in the evolutionary search methodology, no studies have so far attempted to map out the landscape associated with BEC creation. In the global landscape spanned by all possible controls, it is unknown if there is a single optimal strategy for BEC creation, a continuum of connected optimal solutions for a set of equivalent controls realizing physically similar traps (i.e. a surjective mapping), or individual distinct locally optimal strategies of varying quality (see inset of figure 3c) for illustrations). Initial steps in this direction were recently taken by applying Gaussian process optimization to the evaporation ramps in order to determine which parameters would lead to a BEC [68]. The authors concluded that the underlying landscape is trap-free, however, they did not explicitly optimize the size of the BEC and only operated within the space of one of the many strategies that exist for creating a BEC. Below, we discuss several such conventional strategies and their possible connections. In this study, rather than solely focusing on finding the global optimum, we also concentrate on investigating the topology of the landscape in an attempt to find answers to this fundamental question. Experimentally proving that a certain solution is a true optimum is cumbersome, because it requires the faithful reconstruction of the full Hessian [39]. Given the experimental cycle time and the level of shot-to-shot noise [69], we instead concentrate on attempting to disprove optimality of a given solution by identifying a bridge connecting it to a solution of higher quality. First, we will investigate this for a set of standard strategies. Second, we will perform a broader search both using expert remote-optimization and a gamified citizen science approach, the Alice Challenge [23]. In the latter, we will conduct two distinct experiments:

- A *swarm* version of the game (*Alice Swarm Challenge*) aimed at finding optimal solutions. In this mode, the game was open to everyone. Here participants were able to copy other solutions and thereby mimic a human-based implementation of a genetic algorithm.
- A controlled *team* version of the game (*Alice Team Challenge*) specifically aimed at realizing a controlled social science experiment while searching for good solutions. In this mode, access was restricted to 142 participants who were assigned to teams beforehand.

In our experiment [70], we capture  $^{87}\text{Rb}$  atoms in

a trap made of two orthogonal, focused 1064 nm laser beams and a superimposed quadrupolar magnetic field which creates a magnetic field gradient at the position of the atoms and thereby forms a magnetic trap. We evaporatively cool the atoms past the phase transition to a BEC by lowering the intensity of the laser beams as well as the magnetic field gradient. This setting allows for evaporative cooling in two widely used trap configurations. First, making use of only the laser beams a *purely optical* trap can be created, commonly known as a crossed dipole trap (CDT) [71]. Second, a single laser beam can be combined with a weak magnetic trap which is denoted as a hybrid trap [72]. In both cases, the traps are initially loaded from a pure tight magnetic trap [58]. Conventionally, two types of geometrically differing loading schemes are discussed: loading into a large volume trap exhibiting nearly spatially mode-matched type of loading from the magnetic trap into the final trap configuration [63] or a small volume trap with only a small spatial overlap. The latter leads to a “dimple” type loading [73–75] in which a smaller but colder atom cloud is produced. We can directly control the effective volume of the trap by translating the focus of one of the dipole trap beams and thereby changing the size of the beam at the location of the atoms. This inspired us to identify four initial “conventional” trap configurations (BEC creation strategies), the uniqueness of which will be investigated below: a small volume, narrow crossed dipole trap (*NCDT*), a large volume, wide, counterpart (*WCDT*) and similarly a hybrid (*HT*) and wide hybrid trap (*WHT*). At the end of the evaporation process, the traps are turned off and the atoms fall for 86 ms before being imaged with resonant light. The total atom numbers  $N_{\text{tot}}$  and condensed atom numbers  $N_{\text{BEC}}$  are extracted from these images. The optimization landscape topology is determined by the particular constraints imposed [8]. In our case these limitations are vacuum life time, achievable magnetic field gradients, and available beam power.

### A. Line scan optimization

Initially, the control of the time-dependent light and magnetic fields during the loading and evaporation is limited to eight parameters [58]. This is only a restricted representation and later we will relax this condition to allow for full  $(3 \times 90)$ -dimensional optimization set by the programming of the three ramps.

The parameter sets of the four trap configurations are found and optimized locally with respect to  $N_{\text{BEC}}$  in an iterative procedure by performing one-dimensional (1D) *parameter scans*. The result of such a procedure is shown in figure 3a) for the case of the HT. The scans clearly reveal a peak-like structure with a set of optimal solutions, which we will denote 1D-optimal. They hint at a topological structure of the full landscape as shown in inset i) of figure 3c) consisting of four individual peaks. For the above defined conventional trap configurations

(NCDT, WCDT, HT, WHT) we obtain the 1D-optimized values  $N_{\text{BEC}} = (0.53(9), 1.07(5), 1.8(2), 1.1(4)) \cdot 10^6$  [69]. The resulting duration  $T_{\text{ramp}}$  of the whole evaporation (counting from the beginning of loading process) differed for the individual traps and reached  $T_{\text{ramp}} = (2.66, 2.97, 5.56, 6.60)$ s, respectively.

Having established the 1D-optimality of each of the four strategies using scans of individual parameters, we now proceed to investigate the topology of the landscape by searching for interconnecting bridges by simultaneously scanning several parameters. In some cases the mapping between the control parameters and the underlying physics is simple and bridges can be realized by using a simple combination of control parameters. In other cases, the relation can be highly complex. In the following, we will demonstrate the existence of an intuitive connection and then return to the more complex case later in the context of exploring outside the space spanned by the four conventional strategies. Both the low-yield NCDT configuration and the WCDT are types of crossed dipole traps but with different effective volumes dictated by a single parameter, the longitudinal focus position of one of the dipole trapping beams  $x_{\text{focus}}$ . A simple linear interpolation of all the available parameters between the NCDT and the WCDT (cf. equation 1) fails to locate a bridge as illustrated in the inset of figure 3b). This is consistent with the BHW case treated above in which the bridge did not appear until local optimization was performed on the interpolated seeds. Since local optimization is very time consuming in the experimental case, we instead try to extend the search space slightly beyond the simple 1D case. Treating  $x_{\text{focus}}$  independently and introducing a second interpolation parameter realizes an extended 2D-interpolation, which leads to the emergence of a bridge as shown in figure 3b). The necessity of a 2D scan can be understood in terms of the difference between control parametrization and physical subprocesses: The chosen parametrization in terms of different laser beam and magnetic field configurations translate to time dependent trap depths and shapes during the loading and evaporation processes. In this case, the change of the trap depth induced by changing the trap volume has to be counter balanced by the correct choice of the laser intensities involved. This relation is of quadratic nature. The solid red line in figure 3b) marks the position within the given parameter space, which yields the same trap depth at the beginning of the evaporation stage. Changing to a different representation (i.e. a certain combination of parameters) efficiently encapsulating the underlying physics yields a bridge and disproves the local character of the solution strategies involved. We stress that although the bridge was located in a seemingly simple 2D scan, the heuristics introduced for the BHW case of identifying the multi-dimensional search direction by using the parameters interpolating between the established strategies was crucial. These considerations are very much in line with the distinction that Simon and Newell [60] make between task environment (the objec-

tive task) and problem space (the subjective state space that is being searched). Given a good enough problem representation any problem is well defined and simple.

When comparing all other pairs of conventional strategies the choice of parameter combinations for extended interpolation is much harder to motivate physically and simple 1D- and 2D-interpolation fails to locate bridges. A visualization of the relative position of the four initial strategies together with a few of the 1D and 2D interpolations is shown in figure 3c). In addition, extending the interpolation scans between NCDT and HT to a third dimension (which can be seen as a set of 2D interpolation scans with a third parameter varied in each “frame”) did not reveal bridges but instead a novel “frame optimum” which moves frame-by-frame from the HT into the high-dimensional parameter space yielding a slightly higher atom number [58]. This demonstrates that our initial candidate for a global optimum based on 1D-optimization  $N_{\text{BEC}}$  values, the HT, is not a local optimum either when appropriate parameter sets are investigated. One is therefore inclined to view the topology of the landscape closer to what is depicted in inset ii) of figure 3c), where the four conventional strategies are now connected with bridges and another (or many) higher-yield solution such as the “frame optimum” can be identified in the full landscape.

## B. Automated optimization in the landscape

Having established that the global optimum must be found outside the conventional strategies and given the rather long cycle times of the experiment of about 35 s, we abandon the extremely extensive experimental endeavor needed to be able to characterize the remaining two strategies (WHT and WCDT) as potentially true local extrema. Instead, we switch to a more automated search strategy employing numerical optimization. Closed-loop optimization of experiments is a well-known technique also in other research areas, such as the tailoring of radio-frequency fields to control nuclear spins, or the shaping of ultra short laser pulses to influence molecular dynamics (see [77] and references therein). As mentioned above, BEC closed-loop optimization has been explored extensively using random, global methods [64–68]. In addition, the local CRAB algorithm [78] was used to optimize the superfluid to Mott insulator transition [79] and very recently the basis-adaptive variant dCRAB [80] was employed to realize autonomous calibration of single spin qubits [81]. Here we employ the latter due to its local nature (potentially yielding insights into landscape topology) and the ability of the algorithm to avoid getting caught in local traps (in our case, e.g., induced by noise) using periodic reparametrization of the controls.

The main idea of the dCRAB algorithm is to perform local landscape explorations, where the landscape is defined by a parametrization of the control fields via a truncated expansion in a suitable random basis. It has

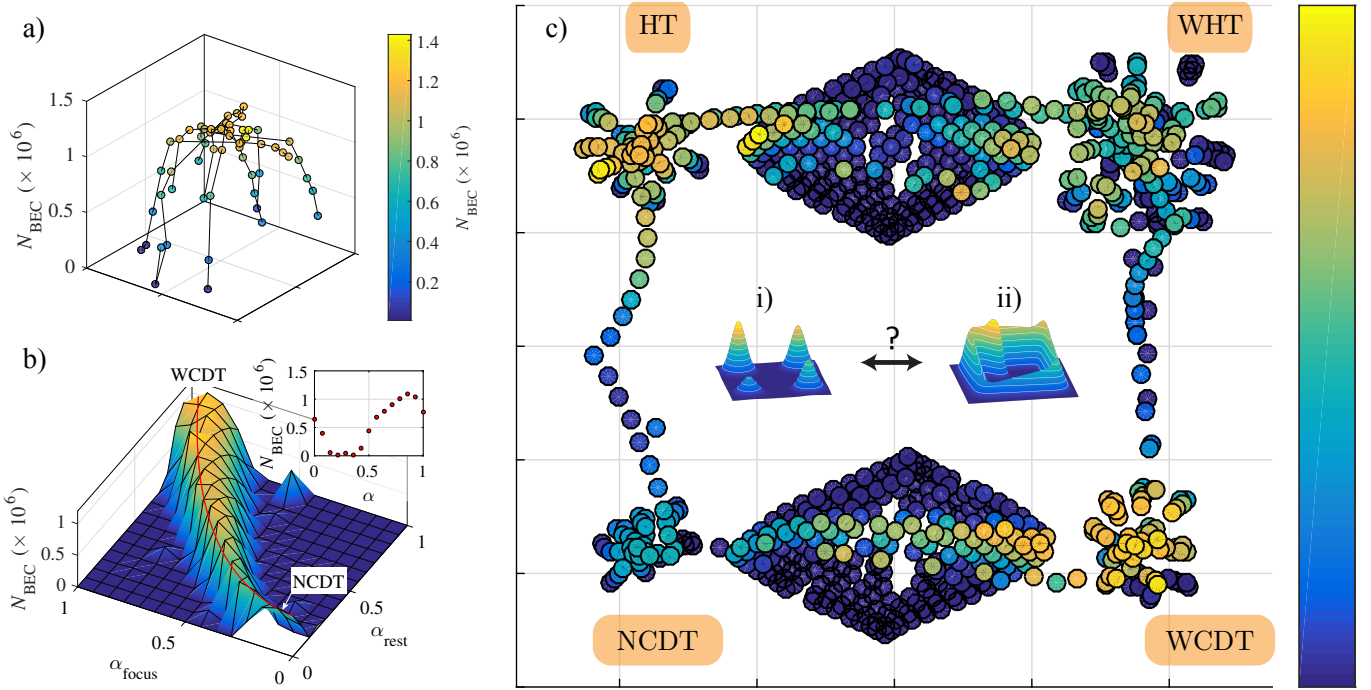


Figure 3. a) 1D parameter scans used to find locally optimized parameters displayed in a 2D tSNE representation exemplarily shown for the hybrid trap. In this case there is no indication for a connection to any of the other “conventional” trap configurations. b) 2D-interpolation between NCDT and WCDT showing a connecting bridge between the two. Along the first dimension the interpolation parameter  $\alpha_{\text{focus}}$  is varied influencing  $x_{\text{focus}}$ . The remaining parameters are scanned synchronously along the second dimension described by the interpolation parameter  $\alpha_{\text{rest}}$ . The solid red line is a simple theoretical estimate of where to find the bridge within the given parameter space. The inset shows a diagonal cut through the landscape and illustrates, a simple linear interpolation with all parameters fails to find a bridge. c) 2D tSNE representation of the landscape showing the variety of different trap configurations that are accessible in our experiment [76]. The plot contains the four main configurations which were scanned and optimized by 1D and 2D parameter scans. Inset i) illustrates the apparent global landscape topology of distinct local optima after performing the 1D parameter scans. However, as inset ii) illustrates, connecting *bridges* were found both between the conventional strategies and to novel high-yield solutions in the high-dimensional search space. For more details, see text.

been shown that the unconstrained dCRAB algorithm converges to the global maximum of an underlying trap-free landscape with probability one [80]. That is, despite working in a truncated space, iterative random function basis changes allow the exploration of enough different directions in the functional space to escape traps induced by the reduced explored dimensionality [82, 83].

Here, the *dCRAB* algorithm is implemented *Remotely* via a cloud interface that can be easily interfaced with computer-controlled experiments and computer simulations (*RedCRAB*, see figure 1c). In our case, the algorithm controls the intensity ramps of the two dipole trap beams as well as a single parameter which represents the value of the magnetic field gradient during evaporation. After simple configuration of the algorithm to accommodate the experimental requirements, the control suite sends the corresponding parameters to the computer in the lab. The experiment is then performed and yields a measurement of the BEC size, quantified by  $N_{\text{BEC}}$ . This number is then sent back to the control suite, which closes the loop by providing an updated set of ramps to be tested in the lab. The process is repeated until con-

vergence or the maximal allowed number of experimental iterations is reached. To utilize the power of the algorithm, an appropriate parametrization was chosen [58]. We ran RedCRAB on the landscape problem presented before, achieving a new maximal  $N_{\text{BEC}} \approx 2.3 \cdot 10^6$  atoms in about one hundred iterations, which exceeds by more than 20 % the result of the HT. This represents a novel solution in the high-dimensional landscape and can be seen as a type of a CDT combined with the magnetic field gradient of the HT. The beam intensities are adjusted to lead to relatively similar trap depths as in the HT. However, especially in the beginning of the evaporation process, the trap is relaxed much faster leading to an overall shorter ramp of  $T_{\text{ramp}} = 4.92$  s [58].

Although the RedCRAB traces out an unsteady path in the optimization landscape, a bridge connecting the HT to this novel solution could be identified [58]. This illustrates that the RedCRAB algorithm is highly effective both at locating novel, non-trivial optimal solutions as well as providing topological information of the underlying landscape.

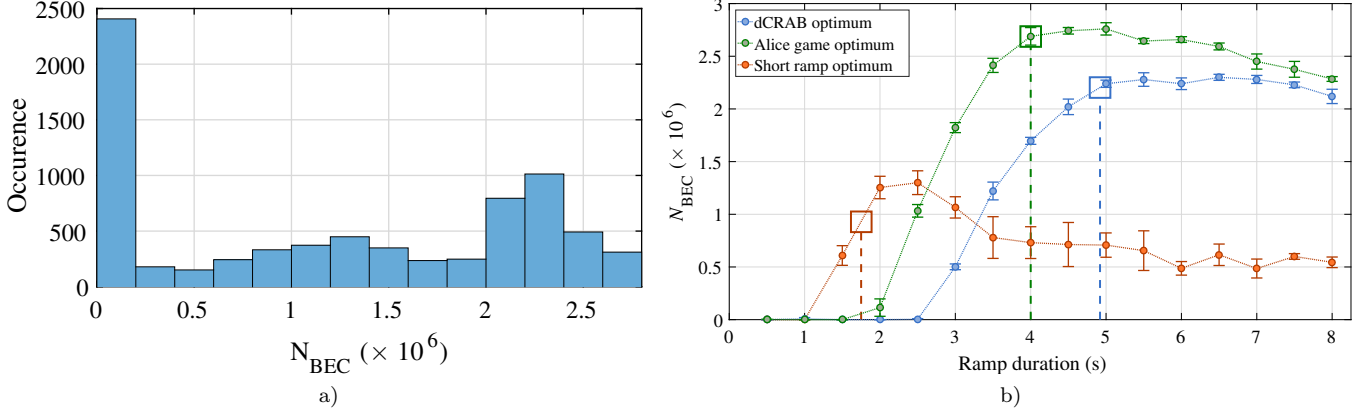


Figure 4. a) Histogram for the achieved number of condensed atoms,  $N_{BEC}$ , for all submitted solutions in the Alice Swarm Challenge. More than 73 % of the submitted solutions were successful and yielded a BEC. b) Sweep of the ramp duration,  $T_{\text{ramp}}$ , for different optimum solutions. The ramp shapes yielded through the RedCRAB optimization and from two Alice Swarm Challenge sessions were scanned as a function of total ramp duration and  $N_{BEC}$  measured. As Alice Swarm Challenge solutions, the ramps resulting in the largest  $N_{BEC}$  and the solution for the shortest set ramp duration were chosen. The data points are obtained by averaging over five repetitions, where the error bars represent the standard deviation. The big squared marks denote  $T_{\text{ramp}}$  during optimization. Note, that the RedCRAB algorithm's control was restricted compared to the one of the players. For details, see text.

### C. Optimizing the creation of Bose-Einstein Condensates with citizen scientists: The Alice Swarm Challenge

One could now exhaustively search the landscape using multi-starting of the RedCRAB algorithm or a global search methodology involving random components. Instead, we now turn to the citizen science approach employing a gamified remote user interface for the general public with the dual purpose of finding optimized solutions as well as conducting controlled social-science experiments. Although several projects offer educational remote access experimentation in physics [84–87], our project is one of the few real-time implementations of an open laboratory allowing actual research experimentation. Other well known examples are the *IBM Quantum Experience* [88] and the project *Quantum in the Cloud* [89]. However, these projects address an audience of “experts” [90, 91], whereas we gamify the problem supported with a didactics strategy to engage the general public.

In our case, we face the challenge of turning the adjustment of laser and magnetic field ramps into an engaging game. We therefore developed a client using the cross-platform engine *Unity* [24] and promoted it through our online community [www.scienceathome.org](http://www.scienceathome.org). As depicted in figure 1e), the ramps are represented by three colored spline curves and are modified by intuitive control points. The total ramp duration was set to a fixed value  $T_{\text{ramp}}$ . The yield in condensed atoms for each solution,  $N_{BEC}$ , is converted into a score in order to provide performance feedback to the players and rank them in a high score list. By making all previous player solutions available for inspection and copying, the setting enables

users to solve problems in a collective fashion. Thus we created an environment where human players can both engage in adaptive search (by manipulating the splines) and emulate a genetic search algorithm since at each turn they can generate solutions by recombining parts of other previous solutions either their own or their peers’.

In the Alice Swarm Challenge, we had roughly 500 individual citizen scientists spanning many countries and levels of education. The submitted solutions were placed in a queue, and, depending on the length of the queue, an estimated process time was displayed. In this way, players could join, submit one or a set of solutions and come back at a later time to review the results. The game was open for participation for one week, 24 hours per day, with brief interruptions to resolve system problems. The players performed unexpectedly well and were able to adapt quickly to changing conditions. As an additional challenge, the game was restarted two to three times per day while changing  $T_{\text{ramp}}$ . In a total of 19 sessions, we covered a range from 1.75 s to 8 s. Discounting four failed sessions, 7577 solutions were submitted. Figure 4a shows the distribution of the attained  $N_{BEC}$ . More than 73 % yielded a BEC.

The largest BEC was found for  $T_{\text{ramp}} = 4$  s and contained about  $2.8 \cdot 10^6$  atoms which set a new record in our experiment. The solutions found by the players were qualitatively different from those found by numerical optimization. Where the RedCRAB algorithm was limited by having only control over the evaporation process and being able to apply only a single specific value for the magnetic field gradient, the players had full control over all ramps throughout the whole sequence of loading and evaporation. This was utilized to create a smoother transition from loading to evaporation. The magnetic field

gradient during evaporation was initially kept at a constant value but relaxed towards the end. Like the automatically optimized solution, the found solutions represent a mixture between HT and CDT [58].

As a concrete example of the difference between obtained solutions, we compare the duration-robustness of the RedCRAB solution and player solutions obtained at short and long durations ( $T_{\text{ramp}} = 1.75$  s and 4 s, respectively) by stretching and compressing the solutions in time. Figure 4b demonstrates that solutions obtained at different durations exhibit dramatically different behavior. For instance, the initial beam intensities are much higher for the short-duration player solution. This leads to a stronger confining trap accommodating the shorter ramp duration. For longer durations this feature seems to be suboptimal. Additionally, the scan reveals that the long-duration player solution is more robust than the RedCRAB solution against reductions in duration. We stress that since it was not a part of the optimization criteria, this behavior is not a reflection of the relative merit of the two methods of optimization. Rather, it highlights the strength of identifying a diversity of solution strategies. This not only gives information about the optimization landscape, but is also potentially an experimental advantage if retrospectively one needs to consider a more complex fitness function. This can incorporate, for example, constraints with respect to ramp duration or laser intensity.

Due to slight changes in experimental performance over the six month [69] data collection period and unequal amount of experimental iterations spent on each, the intention of this experiment was not to realize a stringent competition between automatized and gamified optimization. It is, however, striking that the players were able to compete with numerical optimization in overall performance and also exhibited the ability to adapt to changes in the constraints (such as duration) and conditions (such as experimental drifts). Finally, within the framework of the teams experiment, as we shall see now, the extensive amount of player data forms a valuable resource for social science research.

#### D. Investigating collective problem solving (CPS) with the Alice Team Challenge

The fact that natural science challenges [1, 30–34] can be solved efficiently by the general public is of interest to cognitive and social scientists as a source of insight into the general process of human problem solving. However, data from these projects suffers from the fact that they were not gathered with particular social and cognitive science research questions in mind. Here, we set out a new kind of social science approach, where we investigate *how* a collective of citizens are able to balance local vs. global search in a real-world setting. Such insight is important for future designs of large-scale citizen science investigations of natural science problems and advance

general understanding of the process of individual and collective problem solving.

On an individual level, experiments in the lab have shown that individuals adapt their search based on performance feedback [92] and their search strategies are thus not merely local, nor global [32, 92, 93]. Specifically, if performance is improving, humans tend to make smaller changes (i.e. local search), while if performance is decreasing humans tend to make larger changes (i.e. global search). Collective search is acknowledged to be effective at boosting the efficiency of a search process [94]. Studies in the field of cultural evolution have established that some of the most efficient social learning strategies are to copy the best or most frequent solutions and copy when the situation is uncertain [95–97]. However, potentially constrained by the low dimensionality of the tasks to be solved, these prior studies have primarily focused on simplified situations where individuals have the option to either copy another solution or not [98], with some exceptions [99]. As it is argued in [42], research should not only study option selection, but option generation where participants are not constrained by relatively few options and are allowed to integrate and transform individual and social search information. This enables analysis of *how much* individuals are influenced, rather than merely if they are influenced. In addition, previous work has relied exclusively on participants solving artificially designed tasks. This raises concerns with respect to the external validity of the results: are these general human problem solving patterns or are they merely behaviors elicited by the particular task environment? Finally, previous studies have primarily relied on students at particular universities in a lab setting [44]. Our experimental framework points towards a possible solution to these problems, since we investigate how citizen scientists, engaged in a real world, high-dimensional problem, adapt their search strategies to performance feedback and inspiration from solutions of other players. More specifically, while individuals' ability to do adaptive search may make them uniquely suitable for navigating rugged fitness landscapes as evidenced in previous work [1, 100, 101], we do not know how this adaptive search mechanism plays out in a *collective* search environment where humans not only select between pre-given options but have to generate options while engaging with a high-dimensional, complex problem that is mathematically well defined. This approach has the potential to expand our understanding of human problem solving processes and in particular how humans manage the process of alternating between local and global search behaviours (human adaptive search).

We set out a novel team-based citizen science experiment, which creates new kinds of logistical challenges to solve [58]. For this version of the gamified optimization, small teams of five players each were formed, with every team member being allowed one submission in each of 13 rounds. In each round, every player was asked to submit one solution via the remote interface (see figure 1e). After the solutions from all players in the active team

were collected, they were run on the experiment and results provided to the players. Each round lasted about 180 seconds and in total a 13 round game lasted approximately one hour. Due to no-shows, dropouts, as well as a corrupted session, we analyzed observations from 110 players out of the original 142.

We explicitly instructed participants that they would be working together in a team but that collaboration was possible only through the visibility of team members solutions and scores. In the treatment condition, information regarding how often a certain solution was copied from the previous round by team-members was available to participants, while in the control such information was not available. We conjectured that by presenting participants with this information we could test the occurrence of explicit meta cognitive social learning strategies [102]. More specifically, we hypothesized that because participants could see how many of their teams solutions had been generated by social learning (as opposed to individual search not involving copying) they could compensate, among others, for *under-reliance* on social learning and copy *more* in a given round. In this way we take a first step to study if a collective of human searchers can function as an adaptive global search algorithm, gradually changing their recombination intensity according to their performance as well as the meta-information received.

We analyze the data using generalized linear mixed models with a Gaussian (or Binary with a logit function, where appropriate) error structure and we controlled for individual variance by allowing for a random subject effect. Score related variables are normalized. Models were constructed by forward inclusion and reported effects are within a 95 % confidence interval.

**Results:** Overall, as illustrated in figure 5a), most teams performed surprisingly well compared to the four conventional strategies, especially given the very low number of experimental trials ( $5 \times 13$ ) for each team. Similar to [99], 53 % of all moves were individual, while 41 % involved some form of social learning (see [58] for further descriptive information). Although, as depicted in Fig. 5b), players in the treatment condition relied more heavily on the “copy the best” social learning strategy.

The data show a tendency for people to be conservative as they iterate a given solution. As outlined in Fig. 5d) (see also [58]), on average relatively few players were consistently exploratory and furthermore, players tend to become more conservative as the rounds progress (CI: (-0.12:-0.06), p<0.0001). In order to study how individuals adapt their search, we model the distance from the players’ latest solutions as a function of feedback [58]. As illustrated in Fig. 5c) we find players are more likely to make minor changes to their solutions when they experience performance comparable to the team best versus more major changes when their performance is low comparative to team best feedback (CI: (-1.61: -1.21), p<0.0001), thus supporting former findings on individual adaptive search [92, 93]. Whether players engage in social learning or not depends on previous performance, where

low performance leads to a higher likelihood of engaging in social learning (CI: (-0.92: -0.41), p<0.0001). We also studied social learning in terms of which peer solutions players copy. This behavior follows a similar adaptive mechanism: players will tend to copy more dissimilar solutions, provided they had just experienced low performance (CI:(-1.35:-0.36), p<0.0001). Conversely, with low score differences, players are more likely to copy solutions similar to their own. Our setup also allows to investigate how players manipulate solutions *after* engaging in social learning (i.e. copying another solution), but before submitting their solution. As in pure individual search, players also behave adaptively in this social situation: if they performed better than the previous team-best, their submitted solution will tend to stay closer to the copied solution (CI: (-2.33: -1.34), p<0.0001). Conversely, if their past score is below the same benchmark, their submitted solution will tend to drift further away. A comparison of the rank-based slopes in the graphs illustrating individual and social search showed that the adaptive effect performance induces in subsequent search, appears stronger for individual search (see Fig. S5 and Fig. S6 in [58] for details).

Overall, we created a novel, online gamified interface connecting a real time physics experiment to citizen scientists. The setup provided a unique opportunity to both measure how much a collective of players change their solutions but also have an external measurement of the quality of the solution in the solution space. This enables one going beyond merely claiming human superiority [1, 32] and study *how* human problem solvers are efficient at balancing the trade-off between global and local search.

First, we show that it is possible, via a simple manipulation, to nudge the human players into relying more on social learning strategies, specifically “copy the best”. Considering that previous work [103, 104] argue that human solvers rely *too little* on social learning (i.e. sub-optimally), and thus that an increase in relying on social learning strategies is desirable, this is a promising result. While our finding needs to be confirmed by subsequent experimental tasks that can further isolate the mechanism, it does indicate that by making particular design choices in citizen science tasks, the efficiency of the search process can be significantly improved.

Second, we show how individuals search adaptively depending on their own former performance, thus supporting lab-based studies based on artificial, low-dimensional problems [92, 93], while simultaneously expanding this adaptive mechanism to the realm of social learning. While the nature of the adaptive search mechanism is the same for both individual and social search, we find exploratory evidence for social search inducing less conservativeness for high performers. Finally, our innovative experimental game setup allows a genetic algorithm inspired opportunity to recombine and manipulate existing solutions, going beyond a simple imitation option in each round that simpler setups were constrained by [94, 103].

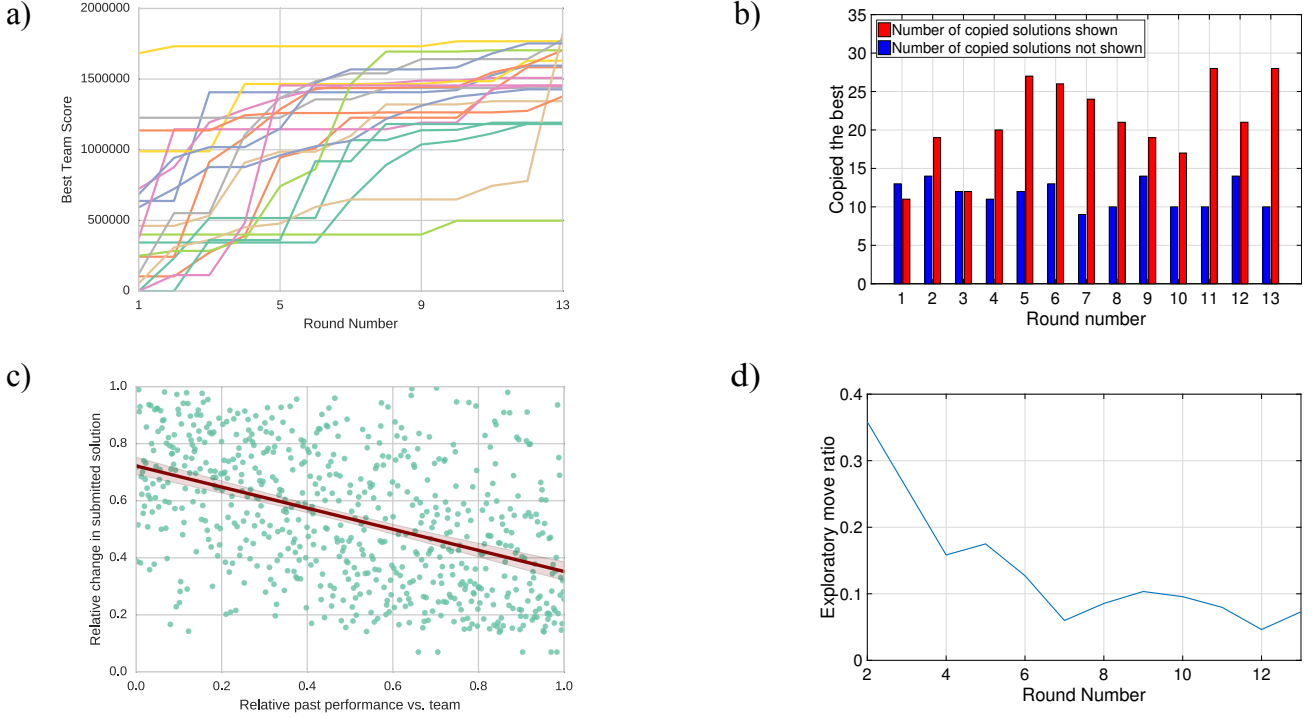


Figure 5. a) Running best performance of Alice Teams with three or more active players. Although human players have had only a very limited amount of tries (13), they still achieve relatively good optimization scores in the Alice Challenge. Overall, all teams but one achieve scores above 1 million. b) Participants in the condition where the meta-information of seeing the number of copied solutions in their team in the previous round was available (red bars), used the “copy the best” social learning strategy more than participants in the condition where this information was not visible (blue bars). A two-sample t-test showed the two to be statistically different ( $p < 0.0001$ ). c) All submissions: How much players edit own solution compared with relative team performance in previous round. The figure includes submissions that did and did not involve any copying. The solutions of players that performed well relative to the team are changed less than players who did not perform well. Distance measure is relative to players own former solution. Both the distance and score measures are ranked within each round with team-best score as a reference point. A 95 % confidence interval is shown. d) Variation of exploration in time. The measure for exploration was derived relative to the entire solution space covered by the players in the Alice Team Challenge. By computing distances from any two solutions submitted in the challenge we have obtained an average distance step of  $\sim 6.13$ . We can classify only  $\sim 9\%$  of players as being on average exploratory, i.e. on average making moves that are above the identified threshold and thus are globally exploratory.

When searching for an optimal solution in a complex, high-dimensional problem space, our exploratory investigation shows that humans don't indiscriminately copy other solutions. They often only copy part of the solution and then further transform the copied solution in an adaptive manner. The fact that these individual and social adaptive search mechanisms systematically depend on the individual searchers' relative performance creates a diverse mixture of search within a collective, shaping the collective balance of local vs. global search and when the collective stops searching. Finally, in presenting the findings, we also point out advantages and potential pitfalls in the path to future implementation of this novel approach.

## E. Conclusion

We have investigated the topology of optimization landscapes in two different systems, namely ultrafast single atom transport and the production of BECs in varying trap configurations. Here, we specifically addressed the question of discreteness of previously identified, seemingly distinct solution strategies. In the single atom transport case, we could locate a bridge between strategies by investigating a set of points interpolated between two known solutions. The fact that extensive random sampling in the vicinity of the solutions failed to identify the bridge hints towards a topology consisting of a densely spaced, sharp peaks and possibly very narrow interconnecting bridges. We interpret the envelope of the maxima of these peaks as a *superlandscape*. We observe that it is slowly varying, which allows us to introduce a

novel *deterministic* global search methodology, GOLSS. We conjecture that the smoothness of the superlandscape is a more general phenomenon in physics and therefore the meta-heuristic, GOLSS, will find application in many areas. A more detailed study of the topology of the superlandscape itself is an interesting topic of future investigation. Identifying multiple not connected extrema here would imply truly distinct strategies for the physical problem.

In the case of BEC production, using the methodology of searching in the vicinity of the direct line connecting known strategies, again bridges could be identified. A novel remote interface that allowed for the first remote

closed loop optimization of such systems was introduced in two contexts: having citizen scientists interact through a gamified remote client and connecting to numerical optimization experts. Both yielded solutions with improved performance compared to the previous best strategies. Finally, the unique experimental citizen science setup enabled us for the first time to experimentally and quantitatively study problem solving “in the wild”, outside the artificial environment of a laboratory, but still in a mathematically well defined manner. We believe these are key factors when designing large-scale experimental set-ups that will allow us to pursue many ambitious social science questions in the future.

- 
- [1] J. J. W. H. Sørensen, M. K. Pedersen, M. Munch, P. Haikka, J. H. Jensen, T. Planke, M. G. Andreasen, M. Gajdacz, K. Mølmer, A. Lieberoth, and J. F. Sherson, *Nature* **532**, 210 (2016).
  - [2] E. A. Baltz, E. Trask, M. Binderbauer, M. Dikovsky, H. Gota, R. Mendoza, J. C. Platt, and P. F. Riley, *Scientific Reports* **7** (2017), 10.1038/s41598-017-06645-7.
  - [3] T. D. Ladd, F. Jelezko, R. Laflamme, Y. Nakamura, C. Monroe, and J. L. O’Brien, *Nature* **464**, 45 (2010).
  - [4] S. J. Devitt, W. J. Munro, and K. Nemoto, *Reports on Progress in Physics* **76**, 076001 (2013).
  - [5] “Sustainable development goals,” <http://www.un.org/sustainabledevelopment/sustainable-development-goals/> (2017).
  - [6] S. Wright, *Proceedings of the Sixth International Congress on Genetics* **1**, 355 (1932).
  - [7] S. Kryazhimskiy, G. Tkacik, and J. B. Plotkin, *Proceedings of the National Academy of Sciences* **106**, 18638 (2009).
  - [8] H. A. Rabitz, M. Hsieh, and C. M. Rosenthal, *Science* **303**, 1998 (2004).
  - [9] H. Rabitz, R.-B. Wu, T.-S. Ho, K. M. Tibbetts, and X. Feng, in *Recent Advances in the Theory and Application of Fitness Landscapes* (Springer Science + Business Media, 2014) pp. 33–70.
  - [10] P. Palittapongarnpim, P. Wittek, E. Zahedinejad, S. Vedaie, and B. C. Sanders, arXiv preprint arXiv:1607.03428 (2016).
  - [11] K. M. Malan and A. P. Engelbrecht, in *Recent Advances in the Theory and Application of Fitness Landscapes* (Springer Science + Business Media, 2014) pp. 103–132.
  - [12] D. A. Levinthal, *Manage. Sci.* **43**, 934 (1997).
  - [13] A. Acerbi, C. Tennie, and A. Mesoudi, *Royal Society open science* **3**, 160215 (2016).
  - [14] G. Dueck, *Journal of Computational Physics* **104**, 86 (1993).
  - [15] J. G. March, *Organization science* **2**, 71 (1991).
  - [16] H. Szu and R. Hartley, *Proceedings of the IEEE* **75**, 1538 (1987).
  - [17] P. Hajela, *AIAA Journal* **28**, 1205 (1990).
  - [18] M. Styblinski and T.-S. Tang, *Neural Networks* **3**, 467 (1990).
  - [19] O. Mersmann, B. Bischl, H. Trautmann, M. Preuss, C. Weihs, and G. Rudolph, in *Proceedings of the 13th annual conference on Genetic and evolutionary computation* (ACM, 2011) pp. 829–836.
  - [20] B. M. Lake, T. D. Ullman, J. B. Tenenbaum, and S. J. Gershman, arXiv preprint arXiv:1604.00289 (2016).
  - [21] O. Russakovsky, J. Deng, H. Su, J. Krause, S. Satheesh, S. Ma, Z. Huang, A. Karpathy, A. Khosla, M. Bernstein, et al., *International Journal of Computer Vision* **115**, 211 (2015).
  - [22] E. Kamar, in *International Joint Conference on Artificial Intelligence* (2016) pp. 4070–4073.
  - [23] “<http://alice.scienceathome.org/>,” (2016).
  - [24] “<https://unity3d.com/>,” (2016).
  - [25] R. Bonney, J. L. Shirk, T. B. Phillips, A. Wiggins, H. L. Ballard, A. J. Miller-Rushing, and J. K. Parrish, *Science* **343**, 1436 (2014).
  - [26] L. von Ahn and L. Dabbish, *Communications of the ACM* **51**, 57 (2008).
  - [27] E. Law and L. von Ahn (ACM Press, 2009) p. 1197.
  - [28] E. Law and L. von Ahn, *Synthesis Lectures on Artificial Intelligence and Machine Learning* **5**, 1 (2011).
  - [29] A. J. Quinn and B. B. Bederson (ACM Press, 2011) p. 1403.
  - [30] C. J. Lintott, K. Schawinski, A. Slosar, K. Land, S. Bamford, D. Thomas, M. J. Raddick, R. C. Nichol, A. Szalay, D. Andreescu, P. Murray, and J. Vandenberg, *Mon. Not. R. Astron. Soc.* **389**, 1179 (2008).
  - [31] D. A. Fischer, M. E. Schwamb, K. Schawinski, C. Lintott, J. Brewer, M. Giguere, S. Lynn, M. Parrish, T. Sartori, R. Simpson, A. Smith, J. Spronck, N. Batalha, J. Rowe, J. Jenkins, S. Bryson, A. Prsa, P. Tenenbaum, J. Crepp, T. Morton, A. Howard, M. Beleu, Z. Kaplan, N. vanNispen, C. Sharzer, J. DeFouw, A. Hajduk, J. P. Neal, A. Nemec, N. Schuepbach, and V. Zimmermann, *Monthly Notices of the Royal Astronomical Society* **419**, 2900 (2012).
  - [32] S. Cooper, F. Khatib, A. Treuille, J. Barbero, J. Lee, M. Beenen, A. Leaver-Fay, D. Baker, Z. Popović, and F. players, *Nature* **466**, 756 (2010).
  - [33] J. Lee, W. Kladwang, M. Lee, D. Cantu, M. Azizyan, H. Kim, A. Limpaecher, S. Gaikwad, S. Yoon, A. Treuille, and R. Das, *Proceedings of the National Academy of Sciences* **111**, 2122 (2014).
  - [34] J. S. Kim, M. J. Greene, A. Zlateski, K. Lee, M. Richardson, S. C. Turaga, M. Purcaro, M. Balkam, A. Robinson, B. F. Behabadi, M. Campos, W. Denk,

- and H. S. Seung, *Nature* **509**, 331 (2014).
- [35] P. R. Freeman, *International Statistical Review / Revue Internationale de Statistique* **51**, 189 (1983).
- [36] D. M. Blei and P. Smyth, *Proceedings of the National Academy of Sciences* **114**, 8689 (2017).
- [37] H. A. Simon, *Psychological Review* **63**, 129 (1956).
- [38] B. R. Newell, D. A. Lagnado, and D. R. Shanks, *Straight choices: The psychology of decision making* (Psychology Press, 2015).
- [39] O. M. Shir, J. Roslund, D. Whitley, and H. Rabitz, *Physical Review E* **89** (2014), 10.1103/PhysRevE.89.063306.
- [40] S. Wold, K. Esbensen, and P. Geladi, *Chemometrics and Intelligent Laboratory Systems* **2**, 37 (1987).
- [41] The novel control software features modular programming and easy remote access. In analogy to “Alice’s Adventures in Wonderland” our system allows the general public to dive into the mysterious quantum world and explore it.
- [42] P. E. Smaldino and P. J. Richerson, *Frontiers in Neuroscience* **6** (2012).
- [43] A. Falk and J. J. Heckman, *science* **326**, 535 (2009).
- [44] J. Henrich, S. J. Heine, and A. Norenzayan, *Behavioral and brain sciences* **33**, 1 (2010).
- [45] A. Lieberoth, *Human Computation* **1** (2014), 10.15346/hc.v1i2.11.
- [46] M. Bukov, A. G. R. Day, D. Sels, P. Weinberg, A. Polkovnikov, and P. Mehta, arXiv:1705.00565 [cond-mat, physics:quant-ph] (2017), arXiv:1705.00565 [cond-mat, physics:quant-ph].
- [47] C. Weitenberg, S. Kuhr, K. Mølmer, and J. Sherson, *Physical Review A* **84**, 032322 (2011).
- [48] A. M. Kaufman, B. J. Lester, M. Foss-Feig, M. L. Wall, A. M. Rey, and C. A. Regal, *Nature* **527**, 1 (2015), arXiv:1507.05586.
- [49] S. E. Sklarz and D. J. Tannor, *Physical Review A* **66**, 11 (2002), arXiv:0209195 [cond-mat].
- [50] S. G. Schirmer and P. de Fouquieres, *New Journal of Physics* **13**, 073029 (2011).
- [51] N. Khaneja, T. Reiss, C. Kehlet, T. Schulte-Herbrüggen, and S. J. Glaser, *Journal of magnetic resonance* **172**, 296 (2005).
- [52] T. Caneva, T. Calarco, and S. Montangero, *Physical Review A* **84**, 022326 (2011).
- [53] S. Machnes, D. J. Tannor, F. K. Wilhelm, and E. Assémat, arXiv:1507.04261 [quant-ph] (2015), arXiv:1507.04261 [quant-ph].
- [54] J. J. W. H. Sørensen, M. O. Aranbu, T. Heinzel, and J. F. Sherson, in preparation (2017).
- [55] E. Zahedinejad, S. Schirmer, and B. C. Sanders, *Physical Review A* **90**, 032310 (2014).
- [56] O. M. Shir, J. Roslund, D. Whitley, and H. Rabitz, arXiv preprint arXiv:1112.4454 (2011).
- [57] L. J. P. van der Maaten and G. E. Hinton, *J. Mach. Learn. Res.* **9**, 2579 (2008).
- [58] See supplementary information.
- [59] L. Mandelstam and I. Tamm, in *Selected Papers*, edited by B. M. Bolotovskii, V. Y. Frenkel, and R. Peierls (Springer Berlin Heidelberg, Berlin, Heidelberg, 1991) pp. 115–123.
- [60] A. Newell, H. A. Simon, and others, *Human Problem Solving*, Vol. 104 (Prentice-Hall Englewood Cliffs, NJ, 1972).
- [61] D. J. Egger and F. K. Wilhelm, *Physical Review Letters* **112** (2014), 10.1103/PhysRevLett.112.240503.
- [62] J. A. Nelder and R. Mead, *The Computer Journal* **7**, 308 (1965).
- [63] W. Ketterle, D. S. Durfee, and D. M. Stamper-Kurn, arXiv:cond-mat/9904034 (1999).
- [64] W. Rohringer, R. Bücker, S. Manz, T. Betz, C. Koller, M. Göbel, A. Perrin, J. Schmiedmayer, and T. Schumm, *Applied Physics Letters* **93**, 2006 (2008).
- [65] W. Rohringer, D. Fischer, M. Trupke, T. Schumm, and J. Schmiedmayer, *Stoch. Optim. - Seeing Optim. Uncertain* **1** (2011), 10.5772/15480.
- [66] I. Geisel, K. Cordes, J. Mahnke, S. Jöllenbeck, J. Ostermann, J. J. Arlt, W. Ertmer, and C. Klempert, *Applied Physics Letters* **102** (2013), 10.1063/1.4808213, arXiv:1305.4094.
- [67] T. Lausch, M. Hohmann, F. Kindermann, D. Mayer, F. Schmidt, and A. Widera, *Applied Physics B* **122** (2016), 10.1007/s00340-016-6391-2.
- [68] P. B. Wigley, P. J. Everitt, A. van den Hengel, J. W. Bastian, M. A. Sooriyanbandara, G. D. McDonald, K. S. Hardman, C. D. Quinlivan, P. Manju, C. C. N. Kuhn, I. R. Petersen, A. N. Luiten, J. J. Hope, N. P. Robins, and M. R. Hush, *Scientific Reports* **6**, 25890 (2016).
- [69] The error bounds represent the standard deviation and are based on benchmarks taken randomly during one month’s period. However, all our experiments presented in the following were conducted over the span of six months and long term drifts of the experimental apparatus were present. RedCRAB optimization and the parameter scans spanned over five months, the Alice challenge and experimental investigation of specific solutions over one month. Individual trap configurations were therefore subjected to an overall drift of up to 14 %. Despite this, the relative yield of different strategies has been investigated with low noise within a short time frame such as in Fig. 8b, and over longer time scales by relating to benchmark sequences.
- [70] M. G. Bason, R. Heck, M. Napolitano, O. Elíasson, R. Müller, A. Thorsen, W.-Z. Zhang, J. Arlt, and J. F. Sherson, arXiv Prepr. (2016), 1607.02934.
- [71] R. Grimm, M. Weidemüller, and Y. B. Ovchinnikov, in *Advances In Atomic, Molecular, and Optical Physics*, Advances In Atomic, Molecular, and Optical Physics, Vol. 42, edited by B. Bederson and H. Walther (Academic Press, 2000) pp. 95–170.
- [72] Y.-J. Lin, A. R. Perry, R. Compton, I. B. Spielman, and J. Porto, *Physical Review A* **79**, 063631 (2009).
- [73] P. W. H. Pinkse, A. Mosk, M. Weidemüller, M. W. Reynolds, T. W. Hijmans, and J. T. M. Walraven, *Physical Review Letters* **78**, 990 (1997).
- [74] D. M. Stamper-Kurn, H.-J. Miesner, A. P. Chikkatur, S. Inouye, J. Stenger, and W. Ketterle, *Physical Review Letters* **81**, 2194 (1998).
- [75] D. Comparat, A. Fioretti, G. Stern, E. Dimova, B. Laburthe Tolra, and P. Pillet, *Physical Review A* **73**, 043410 (2006).
- [76] Note, the displayed data points stem from an older set of measurements, where relative  $N_{BEC}$  between the trap configurations were not represented correctly. Therefore, the labelling of the color scale was omitted.
- [77] C. Brif, R. Chakrabarti, and H. Rabitz, *New Journal of Physics* **12**, 075008 (2010).
- [78] P. Doria, T. Calarco, and S. Montangero, *Physical Review Letters* **106**, 190501 (2011).

- [79] S. Rosi, a. Bernard, N. Fabbri, L. Fallani, C. Fort, M. Inguscio, T. Calarco, and S. Montangero, Physical Review A **88**, 021601 (2013).
- [80] N. Rach, M. M. Müller, T. Calarco, and S. Montangero, Physical Review A **92**, 062343 (2015).
- [81] F. Frank, T. Unden, J. Zoller, R. S. Said, T. Calarco, S. Montangero, B. Naydenov, and F. Jelezko, arXiv:1704.06514 [quant-ph] (2017), arXiv:1704.06514 [quant-ph].
- [82] B. Russell, H. Rabitz, and R.-B. Wu, J. Phys. A: Math. Theor. **50**, 205302 (2017).
- [83] T. Caneva, A. Silva, R. Fazio, S. Lloyd, T. Calarco, and S. Montangero, Phys. Rev. A **89**, 042322 (2014).
- [84] S. Gröber, M. Vetter, B. Eckert, and H.-J. Jodl, European Journal of Physics **28**, S127 (2007).
- [85] Universität der Bundeswehr München, Munich, Germany, “Remotely Controlled Laboratories - RCLs,” <http://rcl-munich.informatik.unibw-muenchen.de/> (2017), Accessed: 2017-09-04.
- [86] S. Khachadorian, H. Scheel, P. de Vries, and C. Thomsen, European Journal of Engineering Education **36**, 21 (2011).
- [87] Department Solid-State Physics, Berlin Institute of Technology, Berlin, Germany, “Remote farm,” <https://remote.physik.tu-berlin.de/en/> (2017), accessed: 2017-09-04.
- [88] IBM, “IBM Quantum Experience,” <http://www-03.ibm.com/press/us/en/pressrelease/49661.wss>, <http://www.research.ibm.com/quantum/> (2016), Accessed: 2017-09-04.
- [89] University of Bristol, “Quantum in the Cloud,” <http://www.bris.ac.uk/news/2013/9720.html>, <http://www.bristol.ac.uk/physics/research/quantum/engagement/qcloud/> (2013), Accessed: 2017-09-04.
- [90] D. Alsina and J. I. Latorre, Physical Review A **94** (2016), 10.1103/PhysRevA.94.012314.
- [91] N. M. Linke, D. Maslov, M. Roetteler, S. Debnath, C. Figgatt, K. A. Landsman, K. Wright, and C. Monroe, Proceedings of the National Academy of Sciences **114**, 3305 (2017).
- [92] S. Billinger, N. Stieglitz, and T. R. Schumacher, Organization Science **25**, 93 (2013).
- [93] O. Vuculescu, Strategic Organization **15**, 242 (2017).
- [94] L. Rendell, R. Boyd, D. Cownden, M. Enquist, K. Eriksen, M. W. Feldman, L. Fogarty, S. Ghirlanda, T. Lilliacrap, and K. N. Laland, Science **328**, 208 (2010).
- [95] T. Morgan, L. Rendell, M. Ehn, W. Hoppitt, and K. Laland, Proceedings of the Royal Society of London B: Biological Sciences **279**, 653 (2012).
- [96] M. Muthukrishna, T. J. Morgan, and J. Henrich, Evolution and Human Behavior **37**, 10 (2016).
- [97] W. Mason and S. Suri, Behavior Research Methods **44**, 1 (2012).
- [98] K. N. Laland, Learning & behavior **32**, 4 (2004).
- [99] M. Derex, R. Feron, B. Godelle, and M. Raymond, in *Proc. R. Soc. B*, Vol. 282 (The Royal Society, 2015) p. 20150719.
- [100] M. Kearns, Science **313**, 824 (2006).
- [101] S. Judd, M. Kearns, and Y. Vorobeychik, Proceedings of the National Academy of Sciences **107**, 14978 (2010).
- [102] C. Heyes, Trends in cognitive sciences **20**, 204 (2016).
- [103] G. Weizsäcker, The American economic review **100**, 2340 (2010).
- [104] R. McElreath, M. Lubell, P. J. Richerson, T. M. Waring, W. Baum, E. Edsten, C. Efferson, and B. Paciotti, Evolution and Human Behavior **26**, 483 (2005).
- [105] K. M. O’Hara, M. E. Gehm, S. R. Granade, and J. E. Thomas, Physical Review A **64**, 1 (2001).

# Supplementary Material: Do physicists stop searches too early? A remote-science, optimization landscape investigation.

## A. Distance map for BHW

In Ref. [1], we introduced a distance map  $D_{ij}$  for two solutions  $i$  and  $j$ , which compares the overlap between two corresponding wave functions  $|\psi_i(x, t)\rangle$  and  $|\psi_j(x, t)\rangle$  at each time step  $t$  for a given total transport time  $T$ :

$$D_{ij} = \frac{1}{T} \int_0^T \langle f_{ij} | f_{ij} \rangle dt, \quad (\text{S1})$$

where  $|f_{ij}(x, t)\rangle = |\psi_i(x, t)\rangle - |\psi_j(x, t)\rangle$  is the difference between the wave functions at each position  $x$ .

## B. Experimental details – Parameter scans

Each trap configuration that is presented in the main text is loaded from a pre-cooled  $^{87}\text{Rb}$  atom cloud prepared in the  $|F = 2, m_F = 2\rangle$  state and trapped in a magnetic quadrupole trap. At this stage, we typically have  $5 \cdot 10^8$  atoms at a temperature of  $\approx 30\text{ K}$ . The experiments of the Alice challenge start from this point. The CDT consists of two perpendicular beams which overlap in the horizontal plane. They have  $1/e^2$  waists of 45 m (beam A) and 85 m (beam B), respectively. The longitudinal focus position  $x_{\text{focus}}$  of beam A can be adjusted, thereby changing its effective waist at the crossing point of the beams. This beam is used to realize HT and WHT. The beams are placed with a vertical offset of around 90 m below the centre of the magnetic trap. An offset magnetic field  $B_{\text{off}}$  in that direction can be used to tune this distance.

For the parameter scans, the intensity ramps  $I(t)$  of the dipole trap beams are described by a function inspired by a simple model of evaporative cooling based on scaling laws [105]

$$\frac{I(t)}{I_i} = \left(1 + \frac{t}{\tau}\right)^{-\beta}. \quad (\text{S2})$$

Here,  $I_i$  is the initial intensity, whereas  $\tau$  and  $\beta$  influence the shape of the ramp. The duration of the ramp is fixed by defining the ratio of initial and final intensity  $I_i/I_f$  for a given  $\tau$  and  $\beta$ . For simplicity, the intensity ratio, as well as  $\tau$  and  $\beta$  are chosen to be the same for the two beams.  $I_i$ , however, is an independent parameter. For the loading process from the magnetic trap into the final trap configuration, the dipole trap beams are regulated to their individual  $I_i$  and the magnetic field gradient is lowered in three linear ramps from 130 G/cm initially to a final value  $B'_f$ , which is retained throughout the evaporation. In total, this leads to eight individual optimization

parameters.

As described in the main text, parameter scans were not only performed in 1D or 2D. In figure S1 the extension of the scan space in the third dimension is presented for parameter sets linearly interpolated between the NCDT and HT. An optimum that moves from frame to frame is revealed and a parameter set is found yielding a slightly higher  $N_{\text{BEC}}$  than in the HT is found. The scan disproves the local character of the HT which was implied by the 1D parameter scans.

## C. Experimental details – Remote optimization

For both the remote optimization with RedCRAB and the Alice challenge, non-optimized configurations were chosen as starting points of the optimization runs. The RedCRAB starting point was close to the HT configuration (see figure S2a). In the Alice challenge at each start of a new round, the highscore list was emptied and filled with low quality solutions yielding typically  $N_{\text{BEC}} \approx (1 - 2) \cdot 10^5$  atoms. In all cases, the position of the translatable focus is fixed such that the waists of both dipole beams overlap. Likewise, the vertical offset magnetic field is fixed to a value compensating the residual background magnetic fields.

In contrast to the previous parametrization of the shape of the laser ramps, RedCRAB (based on the dCRAB algorithm [80]) focuses on a finite set of relevant basis functions that make up a sufficiently good ramp. Here, each of the ramps is composed of a Fourier basis up to the 5<sup>th</sup> harmonics in units of  $2\pi/T_{\text{ramp}}$ , where  $T_{\text{ramp}}$  is the total ramp duration.  $T_{\text{ramp}}$  itself as well as  $B'_f$  during evaporation are chosen to be subject to optimization. The loading procedure of a certain trap configuration is the same predefined sequence described for the parameter scans above. To overcome shot-to-shot fluctuations and thus resulting in an optimization driven and influenced by noise, an adaptive averaging scheme is applied with a stepwise increasing number of averages for higher yields in  $N_{\text{BEC}}$ . Outliers to high  $N_{\text{BEC}}$  are in this way re-evaluated. However, we still keep the number of time-consuming evaluations low at early stages of the optimization which decreases the overall convergence time.

The optimized solution that was found with RedCRAB is a mixture between NCDT and HT.  $B'_f$  resembles closely the one of HT, however 25 % less intensity is used in beam A. This is partially compensated by adding beam B. This results in a trap depth which is about 15 % lower compared to the HT at the beginning of the evaporation. The lowering rate of the trap is comparable in the first part of the evaporation and drops at the end below the one of the HT. At the same time the geometric mean of the trap frequencies ( $\bar{\omega}$ ) is higher. In both cases, the evaporation ends at a similar trap depth and similar  $\bar{\omega}$ . The total ramp duration is with  $T_{\text{ramp}} = 4.92\text{ s}$  shorter than the one of HT.

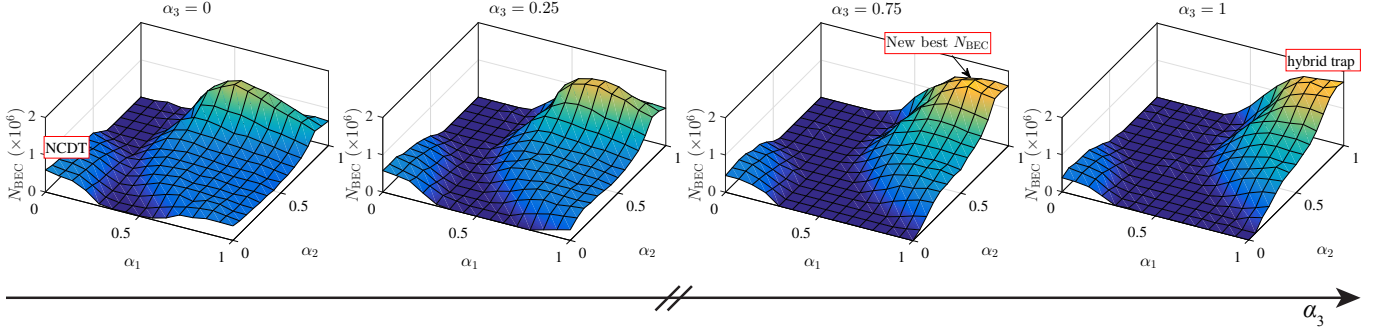


Figure S1. Parameter scan in three dimensions from the NCDT to the HT. Each frame represents a scan point in the third dimension (denoted  $\alpha_3$ ). In frame  $\alpha_3 = 0.75$ , a trap configuration with  $N_{\text{BEC}}$  larger than for the HT is found. This shows that the HT is not a local optimum which is in contrast to the initial indications (see main text).

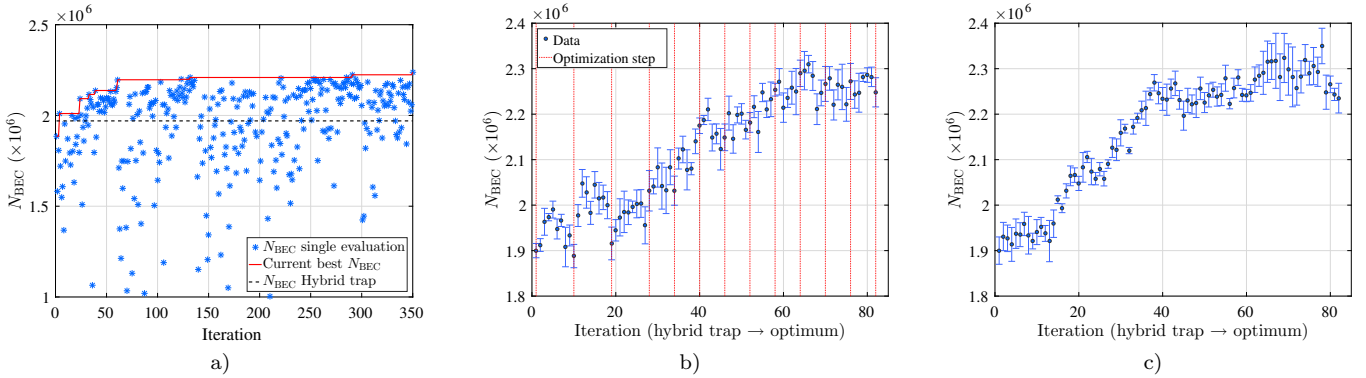


Figure S2. a) Optimization with RedCRAB, where  $N_{\text{BEC}}$  is plotted as a function of optimization algorithm iteration step. The optimization is started from an intermediate point between hybrid trap and NCDT. The blue data points indicate *effective* single evaluations of  $N_{\text{BEC}}$  (note the adaptive averaging scheme that was applied, see text for details). The red solid line denotes the current best  $N_{\text{BEC}}$ . Comparing to the level of the HT (black dashed line),  $N_{\text{BEC}}$  was improved by 20 %. b) Linear interpolation from the HT (first vertical dashed line) through the starting point of RedCRAB optimization in a) (second vertical dashed line) to its optimum (last vertical dashed line). Thereby the ramps between each optimization step (remaining vertical dashed lines) are interpolated. c) Direct linear interpolation between the ramps for the hybrid trap and the found optimum of RedCRAB optimization in a). The error bars in b) and c) represent the standard error for five repetitions.

In the process of reaching this solution, RedCRAB identified of the order of 10 intermediate improved solutions (see steps of the current best  $N_{\text{BEC}}$  depicted as red solid line in figure S2a). If the underlying landscape is sufficiently smooth, one might expect to be able to locate a bridge between the standard strategies and the novel optimum by a linear or possibly non-linear combination of these intermediate solutions. As illustrated in figure S2b) this is nearly but not exactly the case. There are small intervals of decreasing yield. However, a direct linear interpolation between the HT and the novel optimum yields a monotonically increasing bridge (see figure S2c). Thus, the non-monotonicity of the stepwise interpolation is not likely to be caused by ruggedness of the underlying landscape. Rather, a more natural explanation would be that since the local simplex-optimization component of dCRAB is not purely gradient-based it does not necessarily have its axes oriented along the maximal slope and will have a tendency to find a slightly wiggly path

towards the optimum. This increases the chance that experimental noise will occasionally cause the algorithm to find false search directions from which it is slowly recovering in the following iterations. Figure S3 gives a graphical visualization of this phenomenon.

#### D. Experimental details – The Alice Challenge

Around the same time as the development of the remote interface for establishing a connection with RedCRAB, a simplified remote client with a graphical user interface was developed. It allows one to control the dipole beam intensities and the magnetic field gradient via piecewise defined functions. Tests with an undergraduate student and a collaborator situated in the UK were successful. Both were allowed to independently optimize evaporation sequences via this client. Improved solutions were found which lead to the idea of gamifying the task

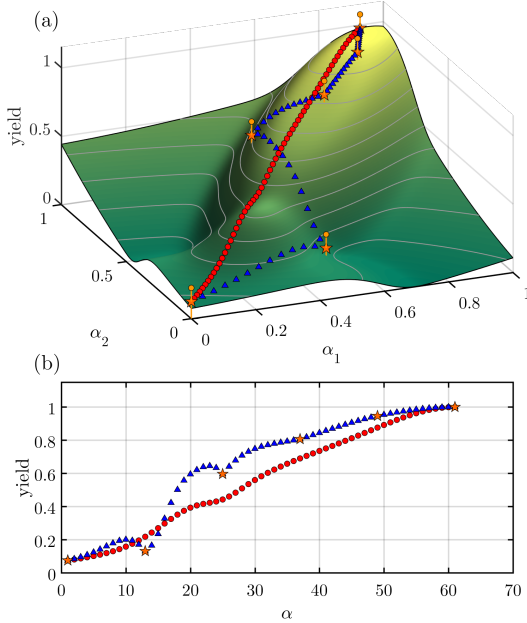


Figure S3. (a) Visualization of an exemplified optimization landscape spanned by parameters  $a$  and  $b$ . In the presence of noise, an optimizer like the RedCRAB algorithm could follow the non-ideal route towards the optimum marked by the orange triangles with error bars. However, following that trace by piecewise interpolation (blue triangles), renders the topology of the landscape visible and results in a non-monotonic trace. Direct linear interpolation (red circles), in this case, exhibits constantly increasing yields. (b) The yield as a function of iteration steps along the paths in (a). It is a possible way to explain the different results of figures S2b and S2c.

of optimizing the evaporation process and give “non-experts” real-time access to our experiment. A prototype version of the game was developed and presented at the National Instruments NIWeek 2016 in Austin, Texas. The event was used for a test-run of the game interface and to acquire a broad potential user base for the actual Alice challenge planned and taking place about a month later.

As described in the main text, the players control the loading sequence as well as the evaporation process through the game interface. In order to account for the high initial and low final parameter values of laser beam intensities and magnetic field gradients, the displayed ramps are represented on a logarithmic and normalized scale. In the Alice Swarm Challenge submitted solutions are placed in a waiting queue. Depending on the length of the queue, an estimated process time is displayed. This allows players to join, submit a single or multiple solutions and come back at a later time to review the achieved score. All results are placed on a highscore list and the players have the possibility to investigate and copy corresponding solutions completely or in parts. This facilitates reproducing working solutions and encourages the players to improve them further. Due to the problem representation, player solutions feature,

in general, a much smoother transition from loading to evaporation than the RedCRAB solutions or the parameter scans with a fixed loading sequence. Knowing the levitation gradient of  $^{87}\text{Rb}$  in  $|F = 2, m_F = 2\rangle$ , one can estimate when the loading of a given trap configuration is finished. In these terms, the loading in the case of the best performing player solutions happens within about 1 s. This is about twice as fast compared to the standard loading sequence described above. Afterwards, the magnetic field gradient is lowered only very slowly and remains nearly constant just below the levitation gradient. This value is about 70 % higher compared to the HT or best performing RedCRAB solution. Only in the last second of the sequence is it relaxed to a value similar as in the HT. The intensities of the dipole beams are lowered after 1 s which is another indicator for the transition from loading to evaporation. Compared to the HT, extremely low intensities are reached at the end of the sequence and it seems that current experimental conditions, such as beam overlap and alignment, are optimally employed.

#### E. Logistical challenges of the Alice Team Challenge

Since participants are not confined to a lab setting nor paid, dropouts can create a major obstacle for such team-based experiments. In abstract terms, there is a  $(1 - E)^N$  probability that all team members will finish all rounds, where  $E$  is the dropout probability and  $N$  is the number of people in the team. The bigger the  $N$  and the more rounds, the bigger the dropout.

We managed this challenge in part by emphasizing the importance to participants of finishing the game as well as increasing the resilience of the team experience by replacing dropouts with bots. Following a recruitment campaign based on snow-balling, 142 participants from around the world committed to taking part in the experiment. Participants selected up to 10 one-hour slots during the week of the challenge. Once the recruitment campaign was over they were randomly assigned to teams, while maximizing the number of complete teams. In incomplete teams, the slots of the missing players were taken by computational agents who would simply reshuffle existing solutions. This was done to minimize the variance dropouts might create between teams. One game session had to be excluded from the data set, because the experiment setup had drifted significantly and thus the evaluation function had been corrupted. All participants gave explicit consent to participate in the study, which was approved by an IRB at Aarhus University.

## F. Variables used in the analysis of individual and social search

Figure S4 shows a histogram of individual highest achieved scores in the Alice Team Challenge. Feedback is defined as the ratio between the individuals previous score and the best team score recorded so far. For individual adaptive search, a similar analysis was conducted using different benchmarks for feedback (i.e. either individual best or second to last submission). These models yielded qualitatively similar results. In the social adaptive learning situation only the social team-best score was considered to be a relevant benchmark. This operationalization follows previous studies that show individuals benchmark their performance against the best performance so far [92, 93]. The search distance is given by the Euclidian distance between consecutively submitted solutions, in the case of individual adaptive search. For social adaptive search, the similarity variable refers to the distance between the copied solution and the solution submitted in the previous time step by the player. The shorter the distance between two solutions, the more similar they are. In Fig. 5c of the main text, Fig. S5 and Fig. S6 feedback and distance measures are rank-based across all players and rounds, while scores are normalized in all modelling efforts. For the reported analysis, the feedback scores are normalized by dividing the individuals current score with the team best so far in the game, leading to corresponding numbers between 0 and 1. Results are robust to varying modelling assumptions, such as standardizing the data, controlling for individual heterogeneity within round or taking round (time) as a fixed effect. The distribution of how often different search strategies were applied is summarized in table I.

The table shows how often players engaged in various types of search moves, combining both treatment conditions. Individual search refers to moves that did not involve any form of copying. Social learning strategies refer to moves that involved copying others. Copy the best refers to copying the entire solution (all three lines) that at the time was the best. Other copying behavior refers to copying any other solution or only partially copying the best (e.g. one or two of the three available lines). If one “shuffled” one got a random combination of existing solutions, i.e. each line could be from different solutions.

**Exploration measure:** The exploration measure was computed by taking the standard deviation of distances between any two solutions in the data set. Players with an average submission to submission distance (across all rounds) above this threshold, were considered to be “exploring”, while players with an average submission to submission distance (across all rounds), were considered to be “exploiting”. We considered average individual behavior since, as highlighted in the main text, players adjust their behavior based on their performance relative to the team best.

**Characteristics of team-participants:** At the end of 13 rounds, participants were redirected and asked to fill in a brief survey. This allowed us to collect a number of demographic variables about the players. We had a response rate of 80 % (89 respondents). The majority of our players were male (69 %), with an average age of 30.1 (st.d = 10.12). With respect to education, 66 % of the participants had obtained a higher education degree and a little over half (53 %) had physics as a subject in their education, after high school. Respondents were from 17 different countries, majority being from Europe or North America.

Table I. Search strategies in Alice Team Challenge

Percentage of overall search strategies		Social learning strategies	
Individual search	53.4%	Copy the best	57.6%
Social learning	41.4%	Other copying behavior	42.4%
Shuffle	5.1%		

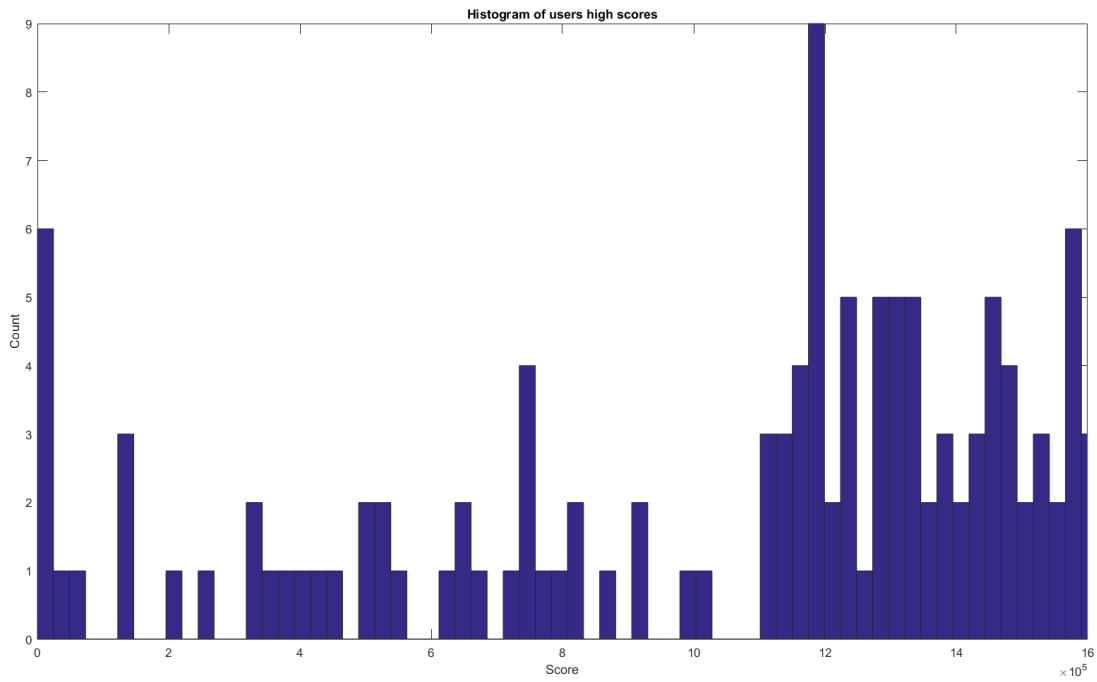


Figure S4. Histogram of individual highest achieved scores in the Alice Team Challenge. Overall, despite a very restricted number of tries, human players achieve relatively good scores. This histogram illustrates that only a handful of players have very low scores (left hand side figure b), while most players achieve scores above the 1 million threshold (right hand side figure b).

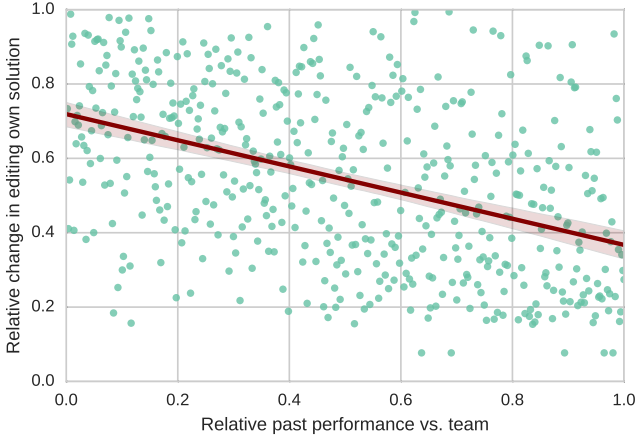


Figure S5. Non-copy events: How much players edit their own solution compared with relative performance in the previous round. The solutions of players that performed well relative to the team are changed less than players who did not perform well. The figure only includes submissions that did not involve any kind of copying. The distance measure is based on distance from the players own previous solution. Both the distance and score measures are ranked within each round with the current team-best score as a reference point. A 95 % confidence interval is shown.

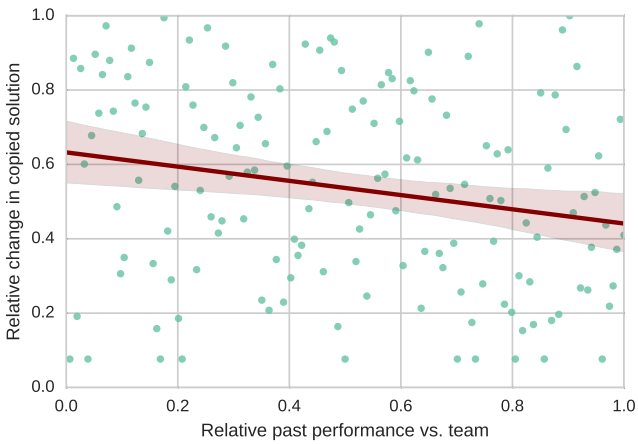


Figure S6. Copy events: How much players edit a solution they have copied compared with relative performance in the previous round. The solutions of players that performed well relative to the team are changed slightly less than players who did not perform well. The figure only includes submissions that involved copying another solution and distance measure is based on distance from copied solution. Both the distance and score measures are ranked within each round with team-best score as reference point. A 95 % confidence interval is shown.